

Efficient coupling of photonic crystal microcavity modes to a ridge waveguide

M. G. Banaee,^{a)} A. G. Pattantyus-Abraham, M. W. McCutcheon,
G. W. Rieger, and Jeff F. Young

Department of Physics and Astronomy, University of British Columbia, Vancouver, British Columbia V6T 1Z4, Canada and Advanced Materials and Process Engineering Laboratory, University of British Columbia, Vancouver, British Columbia V6 T 1Z4, Canada

(Received 2 March 2007; accepted 13 April 2007; published online 7 May 2007)

The unidirectional coupling of a microcavity mode to a ridge waveguide in a slab photonic crystal structure was investigated for the first time. Experimental observation of the coupling efficiency for the signal coupled out of the structure is in good agreement with the result of three-dimensional finite-difference time-domain simulations. The coupling efficiency of the cavity mode to the output channel is $\sim 60\%$. © 2007 American Institute of Physics. [DOI: 10.1063/1.2737369]

Photonic crystal (PhC) microcavities integrated in semiconductor slabs show a promising way to miniaturize nonlinear optical processing for classical and quantum optical applications.¹⁻⁵ The nonlinear sum-frequency generation observed in a microcavity embedded in an InP membrane¹ suggests the possibility of generating parametric down-converted light, which may ultimately help to realize an integrated photonic circuit that incorporates squeezed light, or entangled photon sources suitable for quantum optical information processes.

The utility of these microcavity-based sources strongly depends on the efficiency with which electromagnetic energy can be coupled from the microcavity to single channel waveguides connected to other circuit elements. This feature is especially important for quantum optical applications since the statistics or reduced quantum noise of the nonclassical light generated in microcavities is not well preserved when there is more than one channel in communication with the microcavity.^{6,7} A figure of merit to characterize the efficiency of a cavity for quantum optical applications is the ratio of cavity loss through a desired output channel to the total loss.⁶ To have optimum squeezing in the field quadratures induced in a nonlinear cavity, or to preserve the photon distribution of the nonclassical light generated in these structures, this ratio should be close to 1. In other words, the desired channel should be the main channel that contributes to the cavity loss.

In the current work, a new geometry is introduced to outcouple a photonic crystal microcavity mode through a single-mode ridge waveguide in a silicon-on-insulator (SOI) wafer. The microcavity is freestanding (to increase its quality factor due to better vertical confinement), but the rest of the structure is supported on a SiO₂ layer, which makes it robust. The ridge waveguide is connected by a short segment of a PhC waveguide to the microcavity. The length of the PhC waveguide is kept to a minimum to reduce the strong dispersion that it introduces. Once the light is coupled from the microcavity to the ridge waveguide efficiently, it can be guided anywhere on the integrated photonic chip. In this experiment, a two-dimensional (2D) PhC grating coupler was added to the structure to diffract the light off the chip for

monitoring purposes. To our knowledge, there are just two other experimental reports^{2,8} of a structure for the unidirectional outcoupling of light from a PhC microcavity. The authors in Ref. 2 coupled the microcavity to a one-dimensional (1D) PhC waveguide, with the entire structure made freestanding. They deduced a coupling of 13% from the cavity, via the PhC waveguide, to a tapered optical fiber coupler. Very recently, a coupling efficiency of 40% from a microcavity to a PhC waveguide (with two-hole separation) on a GaAs membrane was reported (Ref. 8), based on a comparison of simulated and measured cavity Q values. They estimated a 90% coupling efficiency when the cavity is tilted with respect to the waveguide axis. The work reported below emphasizes coupling from a freestanding microcavity to a simple silicon ridge waveguide supported on SiO₂: this offers scalability and relatively low loss connectivity over long distances on a SOI chip, with a coupling efficiency of $\sim 60\%$.

Figure 1 shows the geometry of the SOI structure designed and fabricated for the work described below. It consists of a microcavity, a short segment of PhC waveguide, a single-mode ridge waveguide, a tapered waveguide, and a

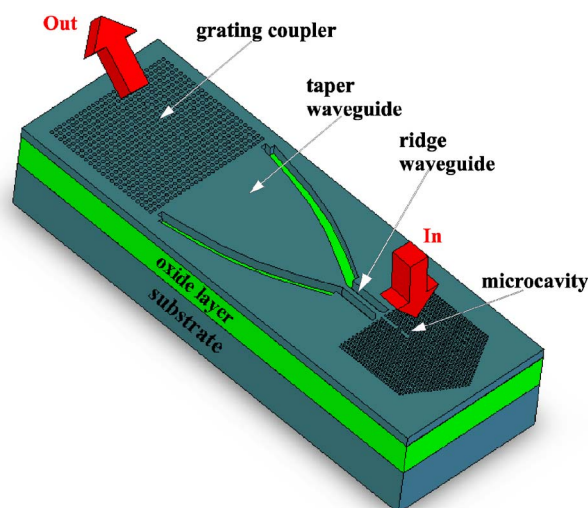


FIG. 1. (Color online) Schematic diagram of Si slab photonic crystal structure in a SOI wafer. All features except the substrate are to scale. There is no oxide layer beneath the microcavity region (see text).

^{a)}Electronic mail: mbanee@physics.ubc.ca

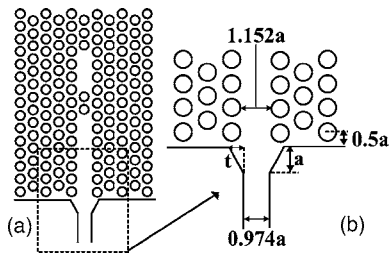


FIG. 2. Three-missing-hole microcavity and its interface with waveguides.

2D grating coupler. The microcavity is a three-missing-hole cavity⁹ in a triangular lattice, with nominal parameters of lattice constant $a=420$ nm and air hole radius $r=0.29a$ [Fig. 2(a)]. The Si slab PhC structure is 196 nm thick and lies on top of a $1.2\ \mu\text{m}$ SiO_2 layer and a $720\ \mu\text{m}$ Si substrate. The PhC waveguide is made by removing six air holes along the Γ -K direction, and it is separated by two holes from the microcavity. The geometry of the interface between the PhC and ridge waveguides is shown in Fig. 2(b). The connection region of the ridge waveguide was tapered to maximize its coupling efficiency to the PhC waveguide segment.¹⁰ The width of the triangular taper in Fig. 2(b) is $t=0.54a$. To ease the coupling of light out of the $10\ \mu\text{m}$ long ridge waveguide, it is connected to a $30\ \mu\text{m}$ long parabolic tapered waveguide (with start and end widths of 400 nm and $14\ \mu\text{m}$, respectively) and a 2D rectangular PhC grating coupler^{11,12} with pitches of $a_{\parallel}=795$ nm (parallel to the waveguide axis), $a_{\perp}=750$ nm, and hole radius of $r_g=244$ nm.

A three-dimensional finite-difference time-domain (FDTD) simulation¹³ is used to characterize the structure and estimate its coupling efficiency. The fundamental mode wavelength and quality factor of the isolated cavity are calculated to be $\lambda=1.520\ \mu\text{m}$ and $Q=4890$, respectively. After adding the waveguides to the microcavity, its Q dropped to 2650, but the frequency of the cavity mode did not change. The simulation showed that by keeping the ridge waveguide and adding back all six-air holes along the PhC waveguide, the Q of the cavity reaches the same value of an isolated cavity. Therefore, removing the air holes of the PhC waveguide allows the waveguide to serve as the main channel of the cavity mode leakage to the environment.

To calculate the coupling efficiency from the microcavity to the uniform silicon waveguide, a 130 fs Gaussian pulse is used to excite the microcavity from the top [see Fig. 1], and the energy buildup in the microcavity and the energy that ultimately passes through the ridge waveguide are calculated. The beam waist radius of the laser on the surface of the structure is set to $1.25\ \mu\text{m}$. The simulation shows that the coupling efficiency from the Gaussian pulsed source to the microcavity and from the microcavity to the waveguide are 0.023 and 0.561, respectively. To calculate the power passing through the waveguide, the Poynting vector along the waveguide axis at a surface $5.70\ \mu\text{m}$ away from the interface of the two waveguides with area $=2 \times 1\ \mu\text{m}^2$ is considered. The energy contained in the microcavity is calculated in a volume $V=\Delta x \times \Delta y \times \Delta z=13\sqrt{3}a \times 36a \times 2.4a$ at the time when the field inside the cavity reaches its maximum. In addition, the simulation shows a 0.169 coupling efficiency from the ridge waveguide to the top of the grating coupler, and the light comes out of the grating coupler at 17° with respect to the normal. Considering all these factors together, the simulation suggests that $\sim 0.22\%$ of the incident Gaussian pulse is

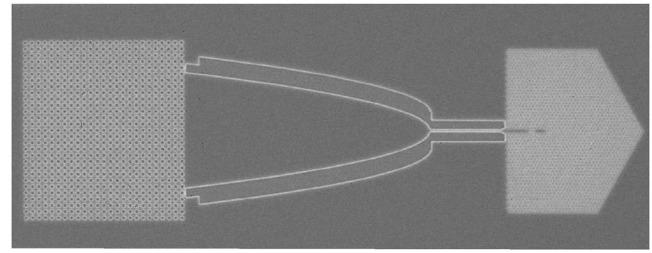


FIG. 3. SEM image of the fabricated microcavity-waveguide structure before the undercutting process.

coupled off the chip via the microcavity mode, waveguides, and grating coupler. This is the quantity that can be compared to the experimental results below, but the key component of this calculation is the $\sim 56\%$ coupling from the microcavity to the ridge waveguide, which is independent of the excitation source and the grating coupler.

A scanning electron microscope, operating at 30 kV, was used to write the pattern in a 500 nm thick ZEP-520A (Zeon Corp.) e-beam resist layer. The pattern was transferred to the Si slab by dry etching with Cl_2 . Figure 3 shows the fabricated structure. In order to maximize the Q of the localized mode, the SiO_2 layer under the microcavity membrane was removed by an undercutting process. In this procedure, $1\ \mu\text{m}$ of photoresist (AZP 4110) was coated on the patterned structure and a square mask was used to cover the waveguides and grating coupler. After exposing the photoresist under a mask aligner and developing, the sample was dipped in a HF solution. Figure 4 shows the undercut microcavity and its interface to the ridge waveguide. Although the end of the ridge waveguide is also undercut (which is unavoidable), it remains single mode.

The microcavity mode frequency and quality factor are measured by a resonant scattering experiment. A 130 fs pulse train of a Spectra-Physics optical parametric oscillator (OPO) laser system is focused on the microcavity from the top half-space by a $100\times$ microscope objective (the beam waist radius of the focused beam was measured by a knife-edge method¹⁴ as $1.25\ \mu\text{m}$), and in the first instance, the light scattered from the microcavity back through the $100\times$ objective is detected with a Bomem Fourier transform spectrometer. Figure 5(a) shows the resonant scattering spectrum of the cavity mode centered at $1.510\ \mu\text{m}$ with $Q=2120$, not far from that predicted by simulation. The Q measured on

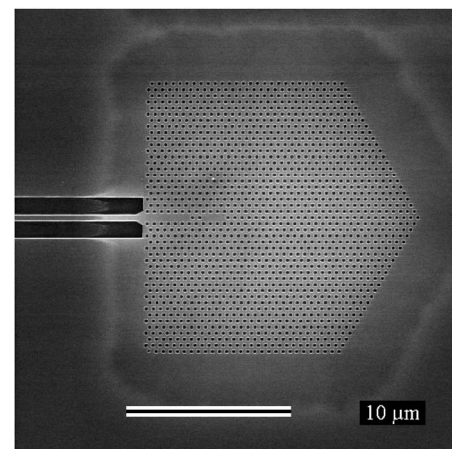


FIG. 4. Undercut is visible as a halo around the microcavity slab.

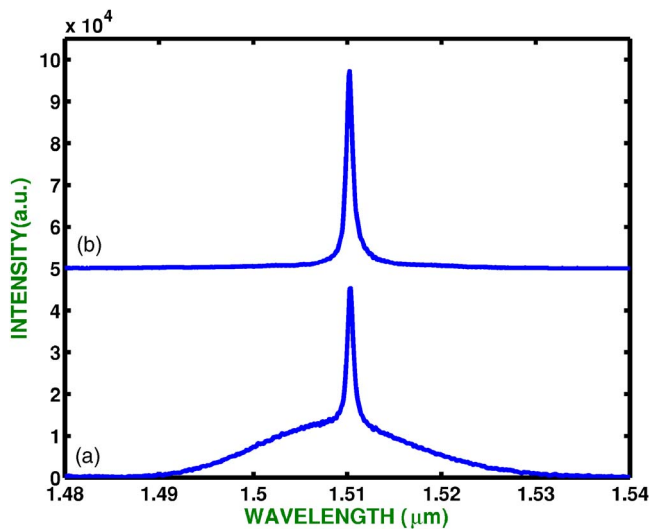


FIG. 5. (Color online) Resonant scattering (a) and background-free signal emanating from the grating coupler (b).

isolated cavities of the same design was $Q=4650$, also close to that predicted by simulation.

To quantitatively compare with the simulation described above, an image of the grating coupler was apertured and sent to the spectrometer. Figure 5(b) shows the signal coming out of the grating coupler from the fabricated SOI structure. In this experiment, $398 \mu\text{W}$ average OPO power focused on the top of the microcavity gives a signal with 600 nW average power out of the grating coupler, giving a measured efficiency of the whole structure of 0.15%.

In conclusion, the calculated total coupling efficiency from the simulation (0.22%) agrees well with the measurement (0.15%). This level of agreement, given the uncertainty in the actual Gaussian spot size, offers confidence that the all-important coupling efficiency from the microcavity to the ridge waveguide is close to that simulated using FDTD ($\sim 56\%$). This is further supported by the measured change in the Q of the waveguide-coupled microcavity ($Q=2100$), as compared to the isolated cavity ($Q=4650$). Additional

simulations suggest that this can be increased by simply shifting the two holes on either end of the cavity (such shifts also affect the Q of an isolated microcavity¹⁵). With a 10% lateral (outward) shift of the holes, the efficiency is increased to 68%. This means that the main channel of cavity loss is through the 1D ridge waveguide and shows a promising geometry to do quantum optical processing. Although this work is done on a SOI structure (which does not have a second-order nonlinearity), the current design could be applied to III-V semiconductor materials.

This work was supported by the Natural Sciences and Engineering Research Council of Canada, the Canadian Institute for Advanced Research, the Canadian Foundation for Innovation, and the British Columbia Knowledge Development Fund.

¹M. W. McCutcheon, G. W. Rieger, I. W. Cheung, J. F. Young, D. Dalacu, S. Frederick, P. J. Poole, G. C. Aers, and R. L. Williams, *Appl. Phys. Lett.* **87**, 221110 (2005).

²P. E. Barclay, K. Srinivasan, and O. Painter, *Opt. Express* **13**, 801 (2005).

³M. Notomi, A. Shinya, S. Mitsugi, G. Kira, E. Kuramochi, and T. Tanabe, *Opt. Express* **13**, 2678 (2005).

⁴A. Badolato, K. Hennessy, M. Atature, J. Dreiser, E. Hu, P. M. Petroff, and A. Imamoglu, *Science* **308**, 1158 (2005).

⁵W. T. M. Irvine, K. Hennessy, and D. Bouwmeester, *Phys. Rev. Lett.* **96**, 057405 (2006).

⁶H. J. Kimble, *Fundamental Systems in Quantum Optics* (Elsevier Science, Amsterdam, 1992), Chap. 10, p. 545.

⁷A. M. Fox, *Quantum Optics: An Introduction* (Oxford University Press, New York, 2006), p. 88.

⁸A. Faraon, E. Waks, D. Englund, I. Fushman, and J. Vuckovic, *Appl. Phys. Lett.* **90**, 073102 (2007).

⁹Y. Akahane, M. Mochizuki, T. Asano, Y. Tanaka, and S. Noda, *Appl. Phys. Lett.* **82**, 1341 (2003).

¹⁰E. Miyai and S. Noda, *J. Opt. Soc. Am. B* **21**, 67 (2004).

¹¹A. Mekis, A. Dodabalapur, R. E. Slusher, and J. D. Joannopoulos, *Opt. Lett.* **25**, 942 (2000).

¹²G. W. Rieger, K. S. Virk, and J. F. Young, *Appl. Phys. Lett.* **84**, 900 (2004).

¹³The FDTD code is provided by Lumerical Solutions Inc.

¹⁴L. Bachmann, D. M. Zzell, and E. P. Maldonado, *Instrum. Sci. Technol.* **31**, 47 (2003).

¹⁵Y. Akahane, T. Asano, B. Song, and S. Noda, *Opt. Express* **13**, 1202 (2005).